Ergonomic Collaboration between Humans and Robots: An Energy-Aware Signal Temporal Logic Perspective

Giuseppe Silano[1], Amr Afifi[2], Martin Saska[1], and Antonio Franchi[2,3,4]

Abstract— **This paper presents a method for designing energy-aware collaboration tasks between humans and robots, and generating corresponding trajectories to carry out those tasks. The method involves using high-level specifications expressed as Signal Temporal Logic (STL) specifications to automatically synthesize task assignments and trajectories. The focus is on a specific task where a Multi-Rotor Aerial Vehicle (MRAV) performs object handovers in a power line setting. The motion planner takes into account constraints such as payload capacity and refilling, while ensuring that the generated trajectories are feasible. The approach also allows users to specify robot behaviors that prioritize human comfort, including ergonomics and user preferences. The method is validated through numerical analyses in MATLAB and realistic Gazebo simulations in a mock-up scenario.**

I. Introduction

In robotics, Multi-Rotor Aerial Vehicles (MRAVs) are popular due to their agility, maneuverability, and versatility with onboard sensors. They have various applications, including contactless or physical interaction with their surroundings [1]. MRAVs are advantageous in scenarios such as working environments at heights, wind turbines, large construction sites, and power transmission lines [2]. They can act as robotic co-workers, carrying tools and reducing physical and cognitive load on human operators, but ergonomics and safety must be considered [3], [4]. However, the use of MRAVs in human-robot interaction is limited compared to ground robots. Object handover is also a well-studied topic.

To enable effective collaboration between MRAVs and human workers, advanced task and motion planning techniques are required to address ergonomic and safety concerns while minimizing the physical and cognitive demands on human operators. Signal Temporal Logic (STL) [5] can provide a framework to express these complex specifications and generate optimal feasible trajectories.

[1]Faculty of Electrical Engineering, Department of Cybernetics, Czech Technical University in Prague, 12135 Prague, Czech Republic (emails: {giuseppe.silano, martin.saska}fel.cvut.cz).

[2]Robotics and Mechatronics Department, Electrical Engineering, Mathematics, and Computer Science (EEMCS) Faculty, University of Twente, 7500 AE Enschede, The Netherlands (emails: {a.n.m.g.afifi, a.franchi}utwente.nl).

[3]Department of Computer, Control and Management Engineering, Sapienza University of Rome, 00185 Rome, Italy (email: antonio.franchi@uniroma1.it).

[4]LAAS-CNRS, Université de Toulouse, 31000 Toulouse, France (email: antonio.franchi@laas.fr).

This work was partially funded by the EU's H2020 AERIAL-CORE grant no. 871479, by the CTU grant no. SGS23/177/OHK3/3T/13, by the Czech Science Foundation (GAČR) grant no. 23-07517S, and by the OP VVV grant no. CZ.02.1.01/0.0/0.0/16 019/0000765.

Handover involves multiple stages: *approach*, *reach*, and *transfer* phases [3], [4]. While some previous studies have examined individual phases, e.g. [6], there is limited consideration of safety and ergonomics in such approaches as well as energy efficiency. For aerial robot-human collaboration in high-risk environments, it is crucial to include these considerations. Additionally, prior works [7], [8] have explored the integration of human comfort and ergonomics in robot planning, but none have considered the context of MRAVs as co-workers with humans.

Some studies use sensors on MRAVs to improve control and planning, with perception-constrained control being a key consideration. For example, [4] proposes a Nonlinear Model Predictive Control (NMPC) formulation that incorporates human ergonomics and comfort while enforcing perception and actuation limits. Other research, such as [3], uses dynamic programming to ensure safety when controlling an aerial manipulator during physical interactions with a human operator. However, these approaches only consider scenarios with a single operator and do not address battery depletion. Regarding motion planning for human-robot handovers, [9] presents a controller automatically generated from STL specifications, while [10] uses probabilistic model-checking to validate a controller for safety and liveness specifications. Neither of these addresses the task assignment and trajectory generation problem to enhance energy-aware human-robot ergonomic collaboration for MRAVs.

This paper presents an energy-aware motion planner that leverages STL specifications to facilitate human-robot collaboration. To this end, a *nonlinear non-convex max-min* optimization problem is formulated, which is addressed using a hierarchical approach that first solves an Integer Linear Programming (ILP) problem. The approach is demonstrated in a power line scenario considering the task of an MRAV performing object handovers as depicted in Fig. 1, where the mission requirements are expressed as an STL formula. Trajectories consider payload capacity limitations and refilling stations for longer-duration operations. Additionally, a method for computing the initial solution for the optimization problem is proposed. Validation is conducted through numerical simulations in MATLAB, while Gazebo simulations demonstrate the approach's effectiveness in a real-world implementation scenario.

II. Problem Description

This paper aims to improve ergonomic human-robot collaboration by designing a trajectory for an MRAV equipped with a manipulation arm to perform object handovers in

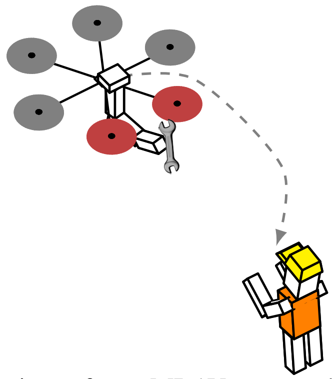

Fig. 1: Illustration of an MRAV approaching a human operator, with gray showing a possible STL optimizer output.

a power line setting. To meet ergonomic requirements, the drone must approach the operator from the front, either from the left or right, from above or below, and never from behind. Additionally, refilling stations are available for the drone to reload tools. The goal is to complete the mission within a specified maximum time frame while meeting dynamic and capability constraints, as well as avoiding obstacles and minimizing energy consumption. To simplify the scenario, we assume that the handover location is a 3D space for each operator, that the MRAV can carry only one tool at a time, and that an onboard low-level controller, e.g. [3], [4], manages the handover procedure. A map of the environment, including obstacles, is assumed to be known in advance.

III. Preliminaries

Let us consider a discrete-time dynamical system $x_{k+1} = f(x_k, u_k)$, where x_{k+1} and $x_k \in \mathcal{X} \subset \mathbb{R}^n$ are the next and current states, respectively, and $u_k \in \mathcal{U} \subset \mathbb{R}^m$ is the control input. Let $f \colon \mathcal{X} \times \mathcal{U} \to \mathcal{X}$ be differentiable in both arguments. With an initial state $x_0 \in \mathcal{X}_0 \subset \mathbb{R}^n$ and a time vector $\mathbf{t} = (t_0, \dots, t_N)^\top \in \mathbb{R}^{N+1}$, we can define the finite control input sequence $\mathbf{u} = (u_0, \dots, u_{N-1})^\top \in \mathbb{R}^N$ to attain the unique sequence of states $\mathbf{x} = (x_0, \dots, x_N)^\top \in \mathbb{R}^{N+1}$ with sampling period $T_s \in \mathbb{R}_{>0}$ and $N \in \mathbb{N}_{>0}$ samples.

Let us consider a Generically Tilted Multi-Rotor (GTMR) model [4] with the world and body frames denoted as $\mathcal{F}_W$ and $\mathcal{F}_B$, respectively, where the origin of $\mathcal{F}_B$ coincides with the Center of Mass (CoM) of the vehicle indicated as $\mathcal{O}_B$. The position, velocity, and acceleration of $\mathcal{O}_B$ in $\mathcal{F}_W$ are denoted as $\mathbf{p}, \mathbf{v}, \mathbf{a} \in \mathbb{R}^3$.

Hence, we define the state and control input sequences of a GTMR model as $\mathbf{x} = (\mathbf{p}^{(1)}, \mathbf{v}^{(1)}, \mathbf{p}^{(2)}, \mathbf{v}^{(2)}, \mathbf{p}^{(3)}, \mathbf{v}^{(3)})^\top$ and $\mathbf{u} = (\mathbf{a}^{(1)}, \mathbf{a}^{(2)}, \mathbf{a}^{(3)})^\top$, where $\mathbf{p}^{(j)}, \mathbf{v}^{(j)}, \mathbf{a}^{(j)}$ are the position, velocity, and acceleration sequences of the vehicle along the j-axis of $\mathcal{F}_W$, respectively. Finally, let us denote with $p_k^{(j)}, v_k^{(j)}, a_k^{(j)}, t_k$ the k-th elements of the sequences $\mathbf{p}^{(j)}, \mathbf{v}^{(j)}, \mathbf{a}^{(j)}$ and vector $\mathbf{t}$, respectively.

A. Signal temporal logic

Definition 1 *(Signal Temporal Logic)*: STL is a concise language for describing real-valued signal temporal behavior [5]. Unlike traditional planning algorithms [11], all mission specifications can be encapsulated into a single formula φ. STL's grammar includes temporal operators, such as *until* ($\mathcal{U}$), *always* ($\Box$), and *eventually* ($\Diamond$), as well as logical operators like *and* ($\wedge$), *or* ($\vee$), and *negation* ($\neg$). These operators act on atomic propositions, which are simple statements or assertions that are either *true* ($\top$) or *false* ($\bot$). An STL formula φ is considered valid if it evaluates to $\top$, and invalid otherwise. More details are available in [5], [12].

Definition 2 *(STL Robustness)*: The satisfaction of an STL formula φ (Def. 1) can be impacted by uncertainties and unexpected events. To ensure a margin of satisfaction, the concept of *robust semantics* for STL formulae has been developed [5], [12]. This *robustness*, ρ, is a quantitative metric that guides the optimization process towards finding the best feasible solution for meeting the statement requirements. It is formally defined using the recursive formulae:

$$
\begin{aligned}
\rho_{p_i}(\mathbf{x}, t_k) &= \mu_i(\mathbf{x}, t_k), \\
\rho_{\neg\varphi}(\mathbf{x}, t_k) &= -\rho_\varphi(\mathbf{x}, t_k), \\
\rho_{\varphi_1 \wedge \varphi_2}(\mathbf{x}, t_k) &= \min\left(\rho_{\varphi_1}(\mathbf{x}, t_k), \rho_{\varphi_2}(\mathbf{x}, t_k)\right), \\
\rho_{\varphi_1 \vee \varphi_2}(\mathbf{x}, t_k) &= \max\left(\rho_{\varphi_1}(\mathbf{x}, t_k), \rho_{\varphi_2}(\mathbf{x}, t_k)\right), \\
\rho_{\Box_I \varphi}(\mathbf{x}, t_k) &= \min_{t'_k \in [t_k + I]} \rho_\varphi(\mathbf{x}, t'_k), \\
\rho_{\Diamond_I \varphi}(\mathbf{x}, t_k) &= \max_{t'_k \in [t_k + I]} \rho_\varphi(\mathbf{x}, t'_k), \\
\rho_{\varphi_1 \mathcal{U}_I \varphi_2}(\mathbf{x}, t_k) &= \max_{t'_k \in [t_k + I]} \Big(\min\left(\rho_{\varphi_2}(\mathbf{x}, t'_k)\right), \\
&\qquad \min_{t''_k \in [t_k, t'_k]} \left(\rho_{\varphi_1}(\mathbf{x}, t''_k)\right) \Big),
\end{aligned}
$$

where $t_k + I$ denotes the Minkowski sum of scalar t_k and time interval I. The formulae comprise *predicates*, p_i, along with their corresponding real-valued function $\mu_i(\mathbf{x}, t_k)$, each of which is evaluated like a logical formula: true if its robustness value is greater than or equal to zero, and false otherwise. Each predicate describes part of the mission specifications, and their robustness values indicate how well the specifications are being met. If all predicates are true, then the result is a numerical value that indicates to what degree the specification is being satisfied. Control inputs that maximize robustness are computed over a set of finite state and input sequences, and the optimal sequence $\mathbf{u}^\star$ is considered valid if $\rho_\varphi(\mathbf{x}^\star, t_k)$ is positive.

Definition 3 *(Smooth Approximation)*: Recent research has proposed smooth approximations for the non-smooth and non-convex robustness measure $\tilde{\rho}_\varphi(\mathbf{x}, t_k)$, which involves the operators $\min$ and $\max$. These approximations can be optimized efficiently using gradient-based methods. One such smooth approximation is the Arithmetic-Geometric Mean (AGM) robustness [13], which we choose as it is more conservative and computationally efficient than the commonly used Log-Sum-Exponential (LSE) [2]. For a full description of the AGM robustness syntax and semantics, see [13].

Definition 4 *(STL Motion Planner)*: By encoding the mission specifications from Sec. II as an STL formula φ and replacing its robustness $\rho_\varphi(\mathbf{x}, t_k)$ with the smooth approximation $\tilde{\rho}_\varphi(\mathbf{x}, t_k)$ (defined in Def. 3), the optimization problem for generating energy-aware trajectories for the GTMR model can be defined as [2]:

$$\begin{array}{ll} \underset{\mathbf{p}^{(j)},\mathbf{v}^{(j)},\mathbf{a}^{(j)},\boldsymbol{\varepsilon}^{(j)}}{\text{maximize}} & \tilde{\rho}_\varphi(\mathbf{p}^{(j)},\mathbf{v}^{(j)}) - {\boldsymbol{\varepsilon}^{(j)}}^\top \mathbf{Q}\, \boldsymbol{\varepsilon}^{(j)} \\ \text{s.t.} & |v_k^{(j)}| \leq \bar{v}^{(j)}, |a_k^{(j)}| \leq \bar{a}^{(j)}, \\ & \|{a_k^{(j)}}^\top a_k^{(j)}\|^2 \leq {\boldsymbol{\varepsilon}_k^{(j)}}^\top \boldsymbol{\varepsilon}_k^{(j)}, \boldsymbol{\varepsilon}_k^{(j)} \geq 0, \\ & \mathbf{S}^{(j)}, \forall k = \{0,1,\ldots,N-1\} \end{array}, \tag{1}$$

where $\boldsymbol{\varepsilon} = (\boldsymbol{\varepsilon}^{(1)}, \boldsymbol{\varepsilon}^{(2)}, \boldsymbol{\varepsilon}^{(3)})^\top$ is the sequence of decision variables $\boldsymbol{\varepsilon}^{(j)}$ representing the bound on the square norm of the MRAV acceleration along each j-axis of the world frame $\mathcal{F}_W$. Also, $\bar{v}^{(j)}$ and $\bar{a}^{(j)}$ denote the upper limits of velocity and acceleration, respectively, and $\mathbf{S}^{(j)}(p_k^{(j)}, v_k^{(j)}, a_k^{(j)}) = (p_{k+1}^{(j)}, v_{k+1}^{(j)}, a_{k+1}^{(j)})^\top$ are the vehicle motion primitives encoding the splines presented in [2]. The energy minimization pass through the term $\boldsymbol{\varepsilon}^\top \mathbf{Q}\, \boldsymbol{\varepsilon}$, where $\mathbf{Q} \in \mathbb{R}^{3N \times 3N}$ such that we have $\boldsymbol{\varepsilon}^\top \mathbf{Q} \boldsymbol{\varepsilon} \geq 0$.

IV. Problem Solution

In this section, we apply the STL framework from Sec. III to formulate the optimization problem presented in Sec. II as a nonlinear non-convex max-min problem. To solve this problem, we generate an initial guess using a simplified ILP formulation that does not account for obstacles, safety, vehicle dynamics, ergonomics, energy minimization, or time specifications. This approach simplifies the search for a global solution. We translate the mission requirements, which include performing object handovers with an MRAV under safety and ergonomic constraints, into the STL formula φ that considers the mission time t_N. The STL formula contains two types of specifications: *safety requirements* that ensure the MRAV stays within a designated area (φ_{ws}), avoids collisions with objects (φ_{obs}), and never approaches the operator from behind (φ_{beh}); and *ergonomic-related objectives* that require the MRAV to visit each human operator (φ_{han}), stay with them for a fixed duration t_{han}, approach them from the front based on their preferences (φ_{pr}), and stop at a refilling station for t_{rs} when its onboard supply of tools is depleted. All mission requirements can be expressed using the STL formula:

$$\varphi = \square_{t_N} \varphi_{\text{ws}} \wedge \varphi_{\text{obs}} \wedge \varphi_{\text{beh}} \bigwedge \lozenge_{t_N} (\varphi_{\text{han}} \wedge \varphi_{\text{pr}} \wedge \varphi_{\text{cap}})\, \mathcal{U}_{t_N} \varphi_{\text{rs}}, \tag{2}$$

with

$$\varphi_{\text{ws}} = \mathbf{p}^{(j)} \in (\underline{p}_{\text{ws}}^{(j)}, \bar{p}_{\text{ws}}^{(j)}), \tag{3a}$$

$$\varphi_{\text{obs}} = \bigwedge_{n}^{\text{obs}} \mathbf{p}^{(j)} \notin ({}^{n}\underline{p}_{\text{obs}}^{(j)}, {}^{n}\bar{p}_{\text{obs}}^{(j)}), \tag{3b}$$

$$\varphi_{\text{beh}} = \bigwedge_{n}^{\text{beh}} \mathbf{p}^{(j)} \notin ({}^{n}\underline{p}_{\text{beh}}^{(j)}, {}^{n}\bar{p}_{\text{beh}}^{(j)}), \tag{3c}$$

$$\varphi_{\text{han}} = \bigwedge_{n}^{\text{ho}} \square_{t_{\text{han}}} \mathbf{p}^{(j)} \in ({}^{n}\underline{p}_{\text{ho}}^{(j)}, {}^{n}\bar{p}_{\text{ho}}^{(j)}), \tag{3d}$$

$$\varphi_{\text{rs}} = \mathbf{p}^{(j)} \in (\underline{p}_{\text{rs}}^{(j)}, \bar{p}_{\text{rs}}^{(j)}), \tag{3e}$$

$$\varphi_{\text{cap}} = \square_{t_{\text{rs}}} (c == 0)\, \mathbf{p}^{(j)} \in (\underline{p}_{\text{rs}}^{(j)}, \bar{p}_{\text{rs}}^{(j)}), \tag{3f}$$

$$\varphi_{\text{pr}} = \bigwedge_{n}^{\text{ho}} \left(\lozenge_{t_N} \bigwedge_{m}^{\text{pr}} \mathbf{p}^{(j)} \in ({}^{n,m}\underline{p}_{\text{pr}}^{(j)}, {}^{n,m}\bar{p}_{\text{pr}}^{(j)}) \right). \tag{3g}$$

Equation (3a) constrains the MRAV's position to remain within the workspace, with minimum and maximum values denoted by $\underline{p}_{\text{ws}}^{(j)}$ and $\bar{p}_{\text{ws}}^{(j)}$, respectively. Equations (3b), (3c), (3d), (3f), and (3e) provide guidelines for obstacle avoidance, operator safety, handover operations, payload capacity, and mission completion, respectively. The payload capacity is represented by $c \in \mathbb{N}_{>0}$. The vertices of rectangular regions identifying obstacles, areas behind the operators, operators themselves, and refilling stations are represented by $\underline{p}_{\text{obs}}^{(j)}$, $\underline{p}_{\text{beh}}^{(j)}$, $\underline{p}_{\text{ho}}^{(j)}$, $\underline{p}_{\text{rs}}^{(j)}$, $\bar{p}_{\text{obs}}^{(j)}$, $\bar{p}_{\text{beh}}^{(j)}$, $\bar{p}_{\text{ho}}^{(j)}$, and $\bar{p}_{\text{rs}}^{(j)}$, respectively. Equation (3g) accounts for the human operators' preferences for the drone's approach. The lower and upper limits for these regions are denoted as $\underline{p}_{\text{pr}}^{(j)}$ and $\bar{p}_{\text{pr}}^{(j)}$, respectively.

A. Initial guess

The resulting nonlinear, non-convex max-min problem is solved using dynamic programming, which requires a well-chosen initial guess to avoid local optima [14]. The strategy for obtaining an appropriate initial guess for the STL motion planner involves simplifying the original problem to an optimization problem with fewer constraints. The resulting ILP problem assigns human operators to the vehicle and provides a navigation sequence for the MRAV. The initial guess considers mission requirements and MRAV payload capacity and refilling operations (φ_{han}, φ_{cap}, and φ_{rs}), but disregards obstacle avoidance and ergonomy requirements (φ_{obs}, φ_{ws}, φ_{beh}, and φ_{pr}), and mission time intervals (t_N, t_{han} and t_{rs}).

The graph used to formulate the ILP is defined by the tuple $G = (\mathcal{V}, \mathcal{E}, \mathcal{W}, \mathcal{C})$, where $\mathcal{V}$ is the set of vertices, consisting of human operators ($\mathcal{T}$), refilling stations ($\mathcal{R}$), and the depot ($\mathcal{O}$) where the MRAV is initially located. The number of elements in $\mathcal{T}$, $\mathcal{R}$, and $\mathcal{O}$ are represented by τ, r, and δ, respectively. The set of edges and their associated weights are represented by $\mathcal{E}$ and $\mathcal{W}$, respectively, where edge weights are modeled using Euclidean distances. To represent the number of times an edge is selected in the ILP solution, an integer variable $z_{ij} \in \mathbb{Z}_{\geq 0}$ is defined for each edge $e_{ij} \in \mathcal{E}$. The variable z_{ij} is limited to the set $\{0, 1\}$ if $\{i, j\} \in \{\mathcal{T}, \mathcal{O}\}$ and $\{0, 1, 2\}$ if $i \in \mathcal{R}$ and $j \in \mathcal{T}$, which ensures that an edge between two human operators is never traversed twice and that the depot is only used as a starting point. The ILP problem is then formulated as:

$$\underset{z_{ij}}{\text{minimize}} \sum_{\{i,j\} \in \mathcal{V},\, i \neq j} w_{ij}\, z_{ij} \tag{4a}$$

$$\text{s.t.} \sum_{i \in \mathcal{V},\, i \neq j} z_{ij} = 2,\ \forall j \in \mathcal{T}, \tag{4b}$$

$$\sum_{i \in \mathcal{T}} z_{0i} = 1, \tag{4c}$$

$$\sum_{i \in \mathcal{T},\, j \notin \mathcal{T}} z_{ij} \geq 2h(\mathcal{T})\,. \tag{4d}$$

In the formulated ILP problem, the objective function (4a) minimizes the distance traversed by the MRAV. Con-

Parameter	Symbol	Value	Parameter	Symbol	Value
Payload capacity	c	$1\,[-]$	Max. velocity	$\bar{v}^{(j)}$	$1.1\,[\mathrm{m/s}]$
Max. acceleration	$\bar{a}^{(j)}$	$1.1\,[\mathrm{m/s}^2]$	Mission time	t_N	$23\,[\mathrm{s}]$
Handover time	t_{han}	$3\,[\mathrm{s}]$	Refilling time	t_{rs}	$3\,[\mathrm{s}]$
Sampling period	T_s	$0.05\,[\mathrm{s}]$	Number of samples	N	$460\,[-]$
Heading operator HO1	ψ_{ho1}	$\pi[\mathrm{rad}]$	Heading operator HO2	ψ_{ho2}	$0[\mathrm{rad}]$

TABLE I: Parameter values for the optimization problem.

straints (4b), (4c) and (4d) ensure that each human operator is visited once, the MRAV begins at the depot and does not return, tours do not exceed payload capacity or are not connected to a refilling station using $h(\mathcal{T})$ [15], respectively. The motion primitives for the MRAV are obtained from the optimal assignment, which is used to generate a dynamically feasible trajectory. The trajectory includes time intervals for handover and refilling (t_{han} and t_{rs}), with fixed rest-to-rest motion between operators and maximum values for velocity and acceleration ($\bar{v}^{(j)}$ and $\bar{a}^{(j)}$). Further details on the motion primitives are provided in [2].

V. Simulation Results

Numerical simulations in MATLAB were used to validate the planning approach, without including vehicle dynamics and trajectory tracking controller. Feasibility was verified in Gazebo with software-in-the-loop simulations [16]. The ILP problem was formulated using the CVX framework, and the STL motion planner used the CasADi library with IPOPT as the solver. Simulations were run on an i7-8565U processor with 32GB of RAM on Ubuntu 20.04. Illustrative videos with the simulations are available at `http://mrs.felk.cvut.cz/stl-ergonomy-energy-aware`.

The object handover scenario outlined in Sec. II was used to evaluate the proposed planning strategy. The simulation scenario consisted of a mock-up environment, with two human operators, one refilling station, and a single MRAV. Parameters and corresponding values used to run the optimization problem are listed in Table I. The heading angle of the MRAV was adjusted by aligning the vehicle with the direction of movement when moving towards the human operator. Once the MRAV reaches the operator, it is assumed that an onboard low-level controller, e.g. [3], [4], handles the handover operation, thus adjusting the heading angle accordingly. The rectangular regions in which the drone was allowed to approach the operator were established taking into consideration the operators' heading, ψ_{ho1} and ψ_{ho2}, as well as their preferred direction of approach (φ_{pr}).

Figure 2 presents a comparison of energy profiles obtained by considering the preferred approach directions of the operators, namely front, right and left, and top to bottom, both with and without the energy term. The energy term is given by $\boldsymbol{\varepsilon}_k^\top \mathbf{Q} \boldsymbol{\varepsilon}_k \geq 0$ and $\|a_k^{(j)\top} a_k^{(j)}\|^2 \leq \boldsymbol{\varepsilon}^{(j)\top} \boldsymbol{\varepsilon}^{(j)}, \boldsymbol{\varepsilon}^{(j)} \geq 0$, as formulated in the problem statement (1). The results demonstrate that the inclusion of the energy term leads to a reduction of energy consumption by approximately 10%.

VI. Conclusions

This paper presented a motion planning framework to improve energy-aware human-robot collaboration for an MRAV

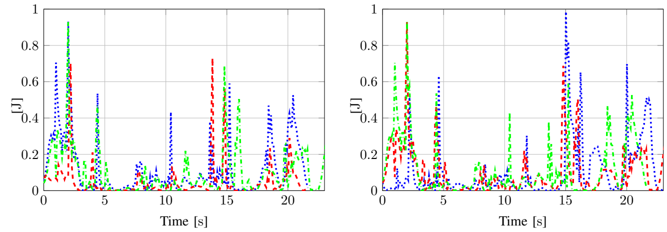

Fig. 2: Normalized energy consumption profiles considering different operators' preferred approach directions, including left and right (blue), front (green), and top to bottom (red). From left to right: the data with and without considering the energy term in the STL motion planner.

with payload limitations and dynamic constraints. The proposed approach uses STL specifications to generate safe and ergonomic trajectories while meeting mission time requirements. An ILP method is introduced to handle the nonlinear non-convex optimization problem. Numerical in MATLAB and realistic simulations in Gazebo confirm the effectiveness of the proposed approach. Future work includes incorporating human operator fatigue and exploring other types of temporal logic languages to adapt the framework for dynamic environments.

References

[1] A. Ollero *et al.*, "Past, Present, and Future of Aerial Robotic Manipulators," *IEEE T-RO*, vol. 38, no. 1, pp. 626–645, 2022.

[2] G. Silano *et al.*, "Power Line Inspection Tasks With Multi-Aerial Robot Systems Via Signal Temporal Logic Specifications," *IEEE RA-L*, vol. 6, no. 2, pp. 4169–4176, 2021.

[3] A. Afifi *et al.*, "Toward Physical Human-Robot Interaction Control with Aerial Manipulators: Compliance, Redundancy Resolution, and Input Limits," in *IEEE ICRA*, 2022, pp. 4855–4861.

[4] G. Corsini *et al.*, "Nonlinear Model Predictive Control for Human-Robot Handover with Application to the Aerial Case," in *IEEE IROS*, 2022, pp. 7597–7604.

[5] O. Maler *et al.*, "Monitoring temporal properties of continuous signals," in *Formal Techniques, Modelling and Analysis of Timed and Fault-Tolerant Systems*. Springer, 2004, pp. 152–166.

[6] J. R. Medina *et al.*, "A human-inspired controller for fluid human-robot handovers," in *IEEE Humanoids*, 2016, pp. 324–331.

[7] E. A. Sisbot *et al.*, "A Human-Aware Manipulation Planner," *IEEE T-RO*, vol. 28, no. 5, pp. 1045–1057, 2012.

[8] L. Peternel *et al.*, "Towards ergonomic control of human-robot co-manipulation and handover," in *IEEE Humanoids*, 2017, pp. 55–60.

[9] A. Kshirsagar *et al.*, "Specifying and Synthesizing Human-Robot Handovers," in *IEEE IROS*, 2019, pp. 5930–5936.

[10] M. Webster *et al.*, "An assurance-based approach to verification and validation of human–robot teams," *arXiv preprint arXiv:1608.07403*, September 2019.

[11] S. M. LaValle, *Sampling-Based Motion Planning*. Cambridge University Press, 2006.

[12] A. Donzé *et al.*, "Robust satisfaction of temporal logic over real-valued signals," in *International Conference on Formal Modeling and Analysis of Timed Systems*. Springer, 2010, pp. 92–106.

[13] N. Mehdipour *et al.*, "Arithmetic-Geometric Mean Robustness for Control from Signal Temporal Logic Specifications," in *IEEE ACC*, 2019, pp. 1690–1695.

[14] D. Bertsekas, *Dynamic programming and optimal control*, Athena Scientific, 2012.

[15] C. Miller *et al.*, "Integer programming formulation of traveling salesman problems," *Journal of the Association for Computing Machinery*, vol. 7, pp. 326–329, 1960.

[16] T. Baca *et al.*, "The MRS UAV System: Pushing the Frontiers of Reproducible Research, Real-world Deployment, and Education with Autonomous Unmanned Aerial Vehicles," *JINT*, vol. 102, no. 26, pp. 1–28, 2021.